Journal of Plastic, Reconstructive & Aesthetic Surgery (2019) 72, 281–289

JPRAS
An International Journal of Surgical Reconstruction
www.JPRASurg.com

Biomechanical behavior of mandibles reconstructed with fibular grafts at different vertical positions using finite element method

Kang-jie Cheng[a], Yun-feng Liu[a,*], Joanne H. Wang[b], Janice C. Jun[c], Xian-feng Jiang[a], Russell Wang[d], Dale A. Baur[c]

[a] *Key Laboratory of E&M (Zhejiang University of Technology), Ministry of Education & Zhejiang Province, 18 Chaowang Rd., Hangzhou, Zhejiang 310014, China*
[b] *Department of Orthopedic Surgery, University Hospitals of Cleveland, Case Medical Center, 11100 Euclid Ave., Cleveland, OH 44016, USA*
[c] *Department of Oral Maxillary Surgery, Case Western Reserve University School of Dental Medicine, 10900 Euclid Ave., Cleveland, OH 44106-4905, USA*
[d] *Department of Comprehensive Care, Case Western Reserve University School of Dental Medicine, 10900 Euclid Ave., Cleveland, OH 44106-4905, USA*

Received 12 September 2017; accepted 28 October 2018

KEYWORDS
Mandibular reconstruction;
Fibular graft;
Bone property;
Finite element method;
Von Mises stress

Summary *Background:* For large mandibular defects, surgical reconstruction using microvascular fibular grafts has advantages over other alternatives in terms of blood supply and good quality of grafted bone. However, the fibular segment is usually lower in height than that of the original mandible, meaning that the vertical positioning of the fibular graft is variable, with different biomechanical consequences on the reconstructed mandible.
Objectives: To use finite element method (FEM) to evaluate stress distribution and displacement of a reconstructed mandible versus an intact mandible under occlusal loads.
Methods: A three-dimensional intact edentulous mandibular bone (Model I) and a reconstructed mandible bone with fibular graft were created from CBCT images. Calculation models were generated with fibular bone graft extracted from the reconstructed mandible of identical length placed into a mimicked defect area on the right-hand side of the mandible at three different vertical positions: superior (Model II), intermediate (Model III), and inferior (Model IV).

* Correspondent author.
E-mail address: liuyf76@zjut.edu.cn (Y.-f. Liu).

https://doi.org/10.1016/j.bjps.2018.10.002

Forces were applied at lower left first molar region and lower left central incisor area. Von Mises stresses and mandibular displacement were calculated as outcome measurements during loadings.

Results: Maximum stress and strain within the reconstructed mandible were identified at the posterior border of the graft and the contralateral condyle. Maximum displacement occurred near the interface of fibular graft and anterior segment of the mandible. Stress distribution in the graft under functional loads is much higher than that in the residual mandibular segments from Models II to IV. The combined average maximum stress from anterior and posterior loads is 10.66 times higher in the mandible with inferiorly positioned graft (Model IV), 8.72 times for superior graft (Model II), and 3.68 times for intermediate graft (Model III) than that in the control group (Model I). The worst displacement result during functional loadings was in the group with fibular graft located at the inferior border of the mandible.

Conclusions: The position of fibular graft placed in the surgical resection site has significant effects on the mechanical behavior of the reconstructed mandible. The fibular graft aligned with the inferior border of the mandible, the most common site designated location by clinicians, has the worst effects on the stress distribution and displacement to the mandibular under functional loads. The fibular graft placed at the intermediate location has the best biomechanics and provides favorable condition for subsequent prosthetic reconstruction.

Introduction

Surgical resection of the mandible often is necessary in treatment of head and neck tumors, infections, trauma or congenital deformities.[1] Facial disfigurement, impairment of chewing, swallowing, speech, and psychologic well-being are challenges for patients who require surgical and prosthetic reconstructions of mandible.[2-8] For large mandibular defects, a fibular flap was first used by Hidalgo in 1989 to surgically reconstruct the mandible,[9] this method has become the treatment of choice because of its many advantages, such as good quality of bone from the fibula, less donor site mobility, and high graft survival based on revascularization.[10,11]

The mandible can experience five types of loading: tension, compression, shear, torsion, and bending. Facture strength of the mandible depends on the direction, location, and type of stress. To be able to resist forces and bending and torsional moments, not only the material properties of the mandible but also its geometrical design is of importance. The mandible is subject to forces produced by the muscles of mastication and by reaction forces acting through the teeth and temporomandibular joints during chewing and clenching. With normal geometry of the mandible, in the longitudinal direction, the mandible is stiffer than in transverse directions, and the vertical cross-sectional dimension of the mandible is larger than its transverse dimension. These features enhance the resistance of the mandible to the relatively large vertical shear forces and bending moments that come into play in the sagittal plane.

Biomechanics of intact mandible have been characterized in the literature;[12-18] however, biomechanical behavior of reconstructed mandibles with various grafting methods is not well understood. Physical models have been used such as animal bone, human cadaveric bone, rapid prototyping, and bone substitutes to provide fracture strength and fatigue information by various mechanical tests at a gross level.[19-21] Most of the literature on mandibular reconstruction using microvascular free fibular flaps deal with surgical techniques, clinical outcomes, and prosthesis designs. Biomechanical analyses of reconstructed mandible with fibular graft under functional loads are lacking because of the complex geometry of the mandible, multidirectional muscle forces, heterogeneous bony structures, and difficulty in obtaining samples for in vivo study.

Finite element method (FEM) is commonly used in industry for numerical mechanical analyses, such as the aeronautical and automotive field. FEM is commonly used to assist design and development of products. Because of its powerful adaptability in calculation, FEM is also suitable for biomechanical analysis of bones, including the mandible.[22,23] Given a high correlation between the FEM and experiments per se, various data within the specimen can be obtained using the FEM calculation. The accuracy of FEM describing the biomechanical behavior of bony specimens has been investigated.[24-27] FEM can provide useful insight into the complex mechanical behavior of mandibles affected by functional loading that could be verified by comparing the calculated data to experimental results on physical models or clinical statistical data.[28,29] Computational models using finite element analysis can predict areas most likely to fail based on internal stress distribution and areas of maximum stress concentration.

A fibula graft is commonly placed at the inferior border of the mandible because of surgeon preference, although it makes a later dental implant placement and tooth restoration more difficult. The diameter of a fibula is significantly less than that of a mandible. The vertical distance between the reconstructed segment and the occlusal plane can be large. This often is a difficult problem for subsequent rehabilitation by an implant-supported prosthesis. The large leverage forces resulting from the high vertical dimension of the prosthetic construction can lead to overloading of the osseointegrated implants and endanger the longevity of the prosthetic restoration. If the fibula is placed more superiorly, it will be easier to place and restore dental implants.

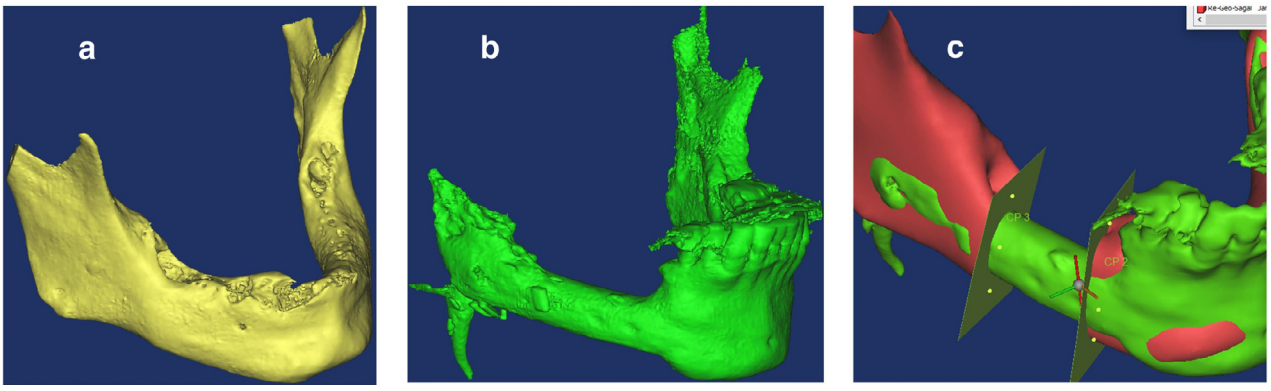

Figure 1 3D models for simulation calculation. (a) Master model of an edentulous mandible; (b) a reconstructed mandible with a fibular graft, which is located in the middle of the bone segments along vertical direction; (c) the two mandibles are registered and a bone defect on the master model was mimicked by resecting and removing a bone segment with two planes and substituted by the fibular graft extracted from the reconstructed mandible by resecting with the same two planes.

The purpose of this work was to investigate the mechanical behavior of reconstructed mandibles with a fibular graft placed at three vertical positions. Three-dimensional (3D) models were constructed based on computerized tomography (CT) images. FEM was used as an analytic tool to study the mechanical behaviors of the reconstructed mandibles. Stress distributions and displacements are the outcome measurements of the reconstructed mandibles during occlusal loadings.

Material and methods

Case information

All CBCT image data of two patients were obtained through a cone beam CT scanner at Case Western Reserve University Craniofacial Image Center, The parameters of the scanner were set at 120 KV, 70 mA, with a field of view of 23 × 16 cm and voxel size of 0.39 mm. A total of 512 images of each patient were saved as DICOM data files. Three mandibular 3D virtual models were created using DICOM files. The first model was created from a normal 50-year-old completely edentulous patient who had multiple extractions 5 months ago without fibular graft (Figure 1a). Virtual alveoloplasty was performed to clean-up thin and sharp bony spikes on the first model. A triangular surface model was refined then converted to a volume mesh FEA model. The second model (Figure 1b) was from a partially edentulous patient who had mandibular reconstruction with fibular bone and fixation plates resulting from resection of squamous cell carcinoma of the floor of the mouth with local bony invasion. Noises from the metal plate of the second model generated by forward and back scatter radiation were manually removed. The mandibular reconstruction plate also was segmented from the second model. A 30 mm portion of the body of the mandible of the first model was segmented, and the resected area was replaced by the fibular graft from the second model. Therefore, a third master model (Figure 1c) with virtual mandibular reconstruction using fibular graft was created by the combination of our first and second models. In an ideal clinical scenario, data from preoperative and postfibular graft of a same mandible would be the best. Practically, it is difficult to come by obtaining the same patient's preoperative and postoperative mandibular DICOM files.

3D reconstruction and meshing

A platform MIMICS (V16.0, Materialise, Belgium) was used to construct the two 3D mandibles based on the DICOM data files. The reconstruction procedure was as follows: first, a threshold for bony tissue segmentation was determined from the value and boundary. The mandible was separated as a sole mask through region of interest extraction. Based on the mask, 3D models represented as triangular mesh (also known as STL file) were created, as shown in Figure 1.

The triangular mesh is only a surface model (Figure 2a). FEM calculation requires volume mesh (tetrahedron) model (Figure 2b). The MIMICS provides a mesh tool named 3-matic (V8.0) for mesh reduction. 3D virtue models can be smoothed and remeshed to form volume meshes with high quality for numerical simulation. Geomagic (V12, 3D system, Rock Hill, SC, USA) software was used to complete the final editing of the triangular model. INP files in Geomagic program can be directly imported to Abaqus (V6.13, Dassault Systèmes, Cedex , France) software, which can create tetrahedron meshes of the models for subsequent simulation and calculation.

Material properties of jaw bone

Bone, consisting of cortical and cancellous parts, is a heterogeneous biomaterial with various degrees of mineralization (various material mechanical properties) that can be detected and translated to different radio-densities from CT images. MIMICS software was used to calculate the material properties of the models such as bone density and Young's modulus based on Hounsfield unit (HU) of CT images. Material properties such as bone density (ρ) and Young's modulus E of each volume mesh of the 3D models were derived from

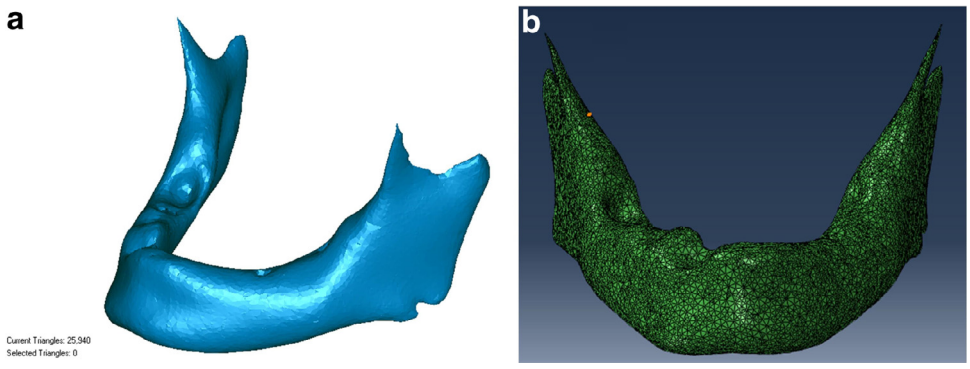

Figure 2 Triangular mesh model and volume mesh model. (a) A triangular mesh model of an intact mandible, a total of 25,940 triangles included; (b) a tetrahedron volume mesh model created from a triangular mesh model.

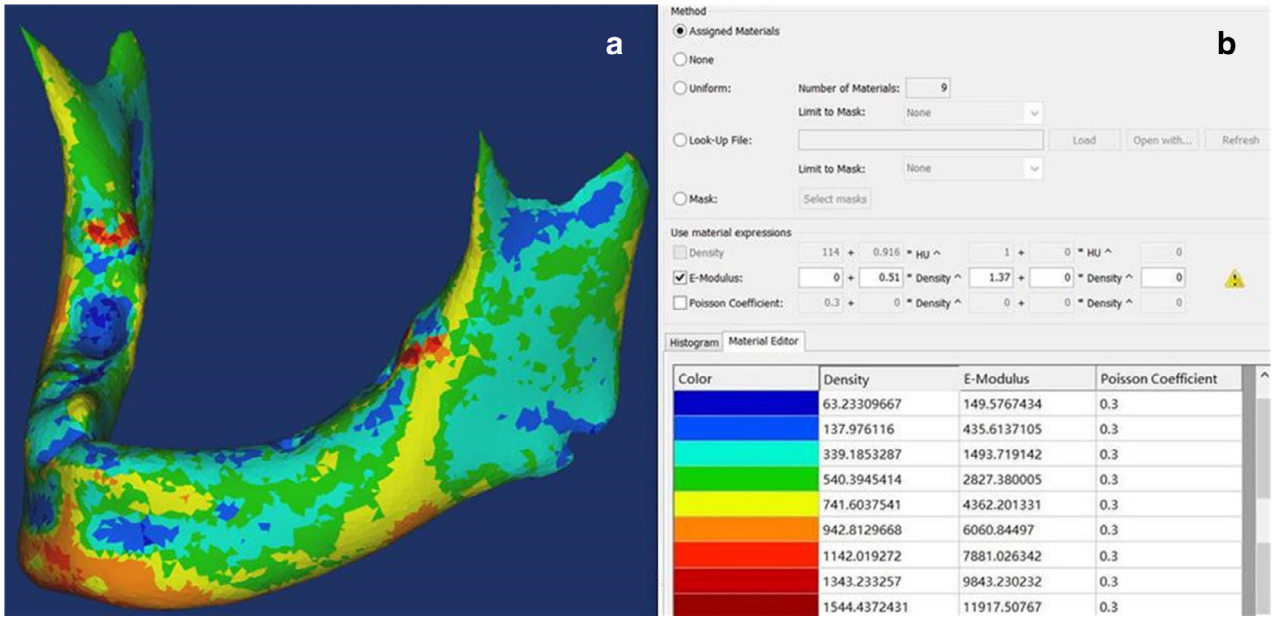

Figure 3 Modeling of material properties. (a) Color-coded model, different colors of the meshes represent different material properties. (b) Material properties were calculated by the CT number, and the color index of the properties was listed.

the following equations:

$$\rho = 114 + 0.916 \times HU \quad (1)$$

$$E = 0.51 \times \rho^{1.37} \quad (2)$$

Figure 3a shows material properties of the master model with different colorations, which correspond to their mechanical properties. Figure 3b lists modulus and density, which are derived from Eqs. (1) and (2). This model can be exported from MIMICS into Abaqus through INP file for subsequent simulations and calculations. The material properties of fibular graft were also calculated by the same method.

Calculation models with graft at various positions

A defect on the right-hand side of the mandibular was created with MIMICS and replaced with either the original bone segment as a control or a fibular graft at various vertical positions. Four tested models were created: Model I, the original segment was used (Figure 4a); Model II, a fibular graft was placed at the superior position between two residual mandibular segments (Figure 4b); Model III, a fibular graft was placed at the intermediate vertical position (Figure 4c); Model IV, a fibular graft was placed at the inferior border of the mandible (Figure 4d).

Loading and constraints

To simulate a static status with loading forces during mastication, two TMJ condyles could be fixed on all six freedoms, as references 30-32. Figure 5 shows occlusal loadings applied to the control and the experimental groups at two locations of the mandibles: Location ① - lower left first molar and Location ② - lower left central incisor. Forces were perpendicular to the occlusal table (*Z* axis). Mandibular condyles were fixated to prevent movement in any

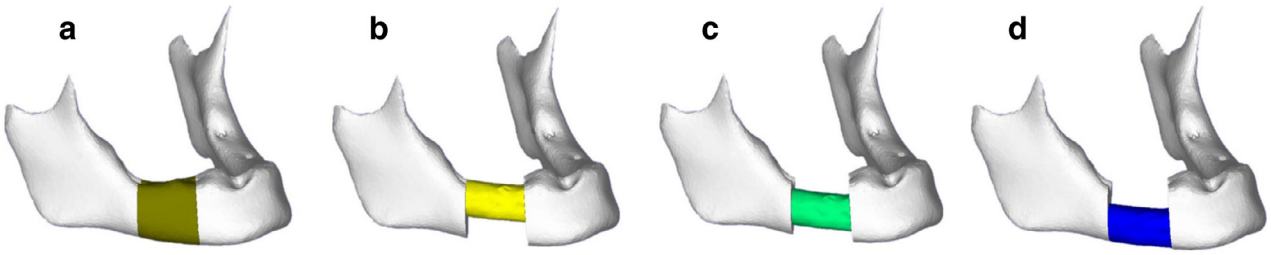

Figure 4 Model groups. (a) Model I: original segment from the intact mandible; (b) Model II: fibular graft is placed at the superior position flush with the adjacent mandibular segments; (c) Model III: fibular graft is placed at the intermediate vertical position; (d) Model IV: fibular graft is placed at the inferior position flush with the adjacent mandibular segments.

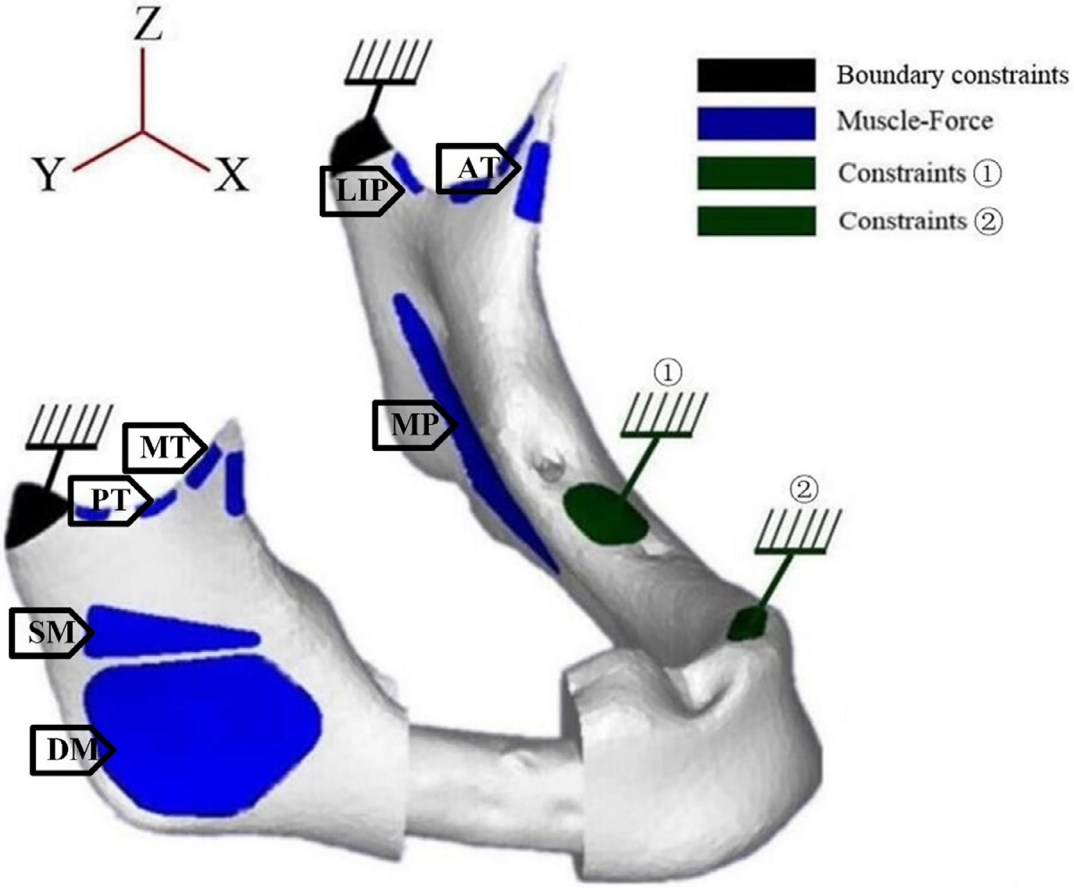

Figure 5 Loading and boundary constraints on mandible. Condyles fixated in all directions (black), origins of mandibular muscles (blue), and occlusal loading (green).
Note. SM is superficial masseter, DM is deep]masseter, MP is medial pterygoid, AT is anterior temporal, MT is middle temporal, PT is posterior temporal, and LIP is lateral inferior pterygoid.

direction (Figure 5, black).[30] To create more accurate models, jaw opening and closing muscles were added to the model design. Muscles origins are labeled with blue in Figure 5. The direction and magnitude of muscle forces were based on data from Nelson[33] for FEM calculations. Tables 1 and 2 are the values of muscle forces and directions of forces in *x*, *y*, *z* directions. Comparing to closing muscles, reactions from the opening masticatory muscles, such as digastric and mylohyoid muscle, are too small that would not significantly affect the calculation results in the static status. Therefore, there was no need to integrate the opening muscles in the calculation model.[30-32]

Results

The outcome measurements from FEM results are stresses, strains, and displacements within the mandibles and the fibular bone graft. Figure 6 shows the distributions of Von Mises stress (MPa), strains (%), and the amount of

Table 1 Muscle force with constraint, loading ① - at first molar area.

Muscle	Muscle weight (N)	Scaling factors		Unit vector coordinates		
		Working side	Balancing side	*X*	*Y*	*Z*
Superficial masseter	190.40	0.72	0.60	−0.21	−0.42	+0.89
Deep masseter	81.60	0.72	0.60	−0.55	+0.36	+0.76
Medial pterygoid	174.80	0.84	0.60	+0.49	−0.37	+0.79
Anterior temporal	158.00	0.73	0.58	−0.15	−0.04	+0.99
Middle temporal	95.60	0.66	0.67	−0.22	+0.50	+0.83
Posterior temporal	75.60	0.59	0.39	−0.21	+0.86	+0.47
Lateral inferior pterygoid	66.90	0.30	0.65	+0.63	−0.76	−0.17

Table 2 Muscle force with constraint, loading ② - at central incisor.

Muscle	Muscle weight (N)	Scaling factors		Unit vector coordinates		
		Working side	Balancing side	*X*	*Y*	*Z*
Superficial masseter	190.40	1.00	1.00	−0.21	−0.42	+0.89
Deep masseter	81.60	1.00	1.00	−0.55	+0.36	+0.76
Medial pterygoid	174.80	0.76	0.76	+0.49	−0.37	+0.79
Anterior temporal	158.00	0.98	0.98	−0.15	−0.04	+0.99
Middle temporal	95.60	0.96	0.96	−0.22	+0.50	+0.83
Posterior temporal	75.60	0.94	0.94	−0.21	+0.86	+0.47
Lateral inferior pterygoid	66.90	0.27	0.27	+0.63	−0.76	−0.17

Note. The force of each muscle was determined by the muscle weight multiplied by the scaling factors and the three-unit vector coordinates across the area of attachment. All coordinates are referenced to a global Cartesian coordinate system, where the *XY*-plane is the frontal plane, *XZ* represents the orientation of the occlusal plane, and the *YZ*-plane is orthogonal to both *XY* and *XZ*.

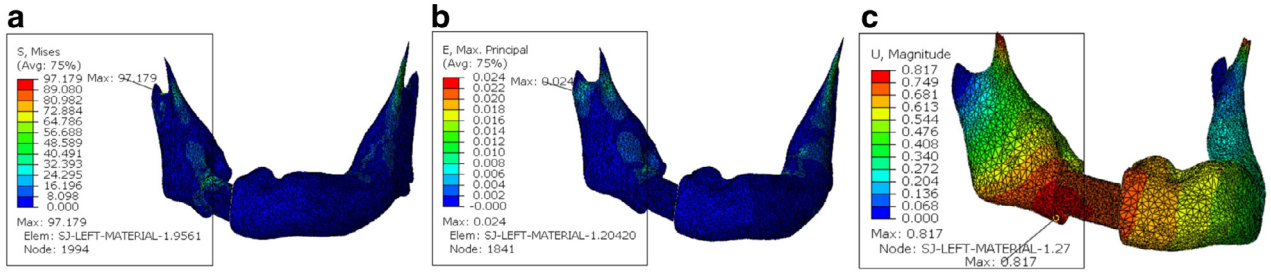

Figure 6 FEM results of Model III with left molar loading. (a) Von Mises stress distribution, (b) principal strain distribution, and (c) displacement of mandible and graft.

mandibular displacement (mm) of the mandible of Model III under occlusal loading at left molar area. The maximum stress and strain are identified at both the posterior border of the graft and the contralateral condyle area. Maximum displacement occurs near the interface of fibular graft and anterior segment of the mandible.

Figure 7 shows the Von Mises stress distributions in the mandible and the fibular bone under occlusal loadings at the left molar area as well as at the left central incisor. Under both loading conditions, maximum stresses among the four groups show the same pattern. Grafts placed at the inferior border of the mandible always yield the worst results. The superior location, middle location, and the control group are progressively better, in that order.

Tables 3 and 4 summarize the results of maximum Von Mises stress and the amount of mandibular displacement under loading ① and loading ② conditions.

Discussion

Common method in the literature using FEM has tended to assume that the mandible is isotropic rather than anisotropic to simplify the calculation. In this study, we derive various bone properties throughout the mandible (Figure 3) and integrate force directions of seven masticatory muscles (Figure 5) in the modeling system. We intentionally choose a completely edentulous model for the FEM analysis of fibular graft because of the difficulty of modeling tooth structures (three layers: enamel, dentine, and pulp chamber) and periodontal ligament. Our goal was to evaluate the mechanical behavior of the graft and native bone without the compounding factor from the teeth. The model provides more accurate FEM data to analyze the internal stress patterns throughout the mandible, the effect of changes in loading, and prediction of areas of likely failure.

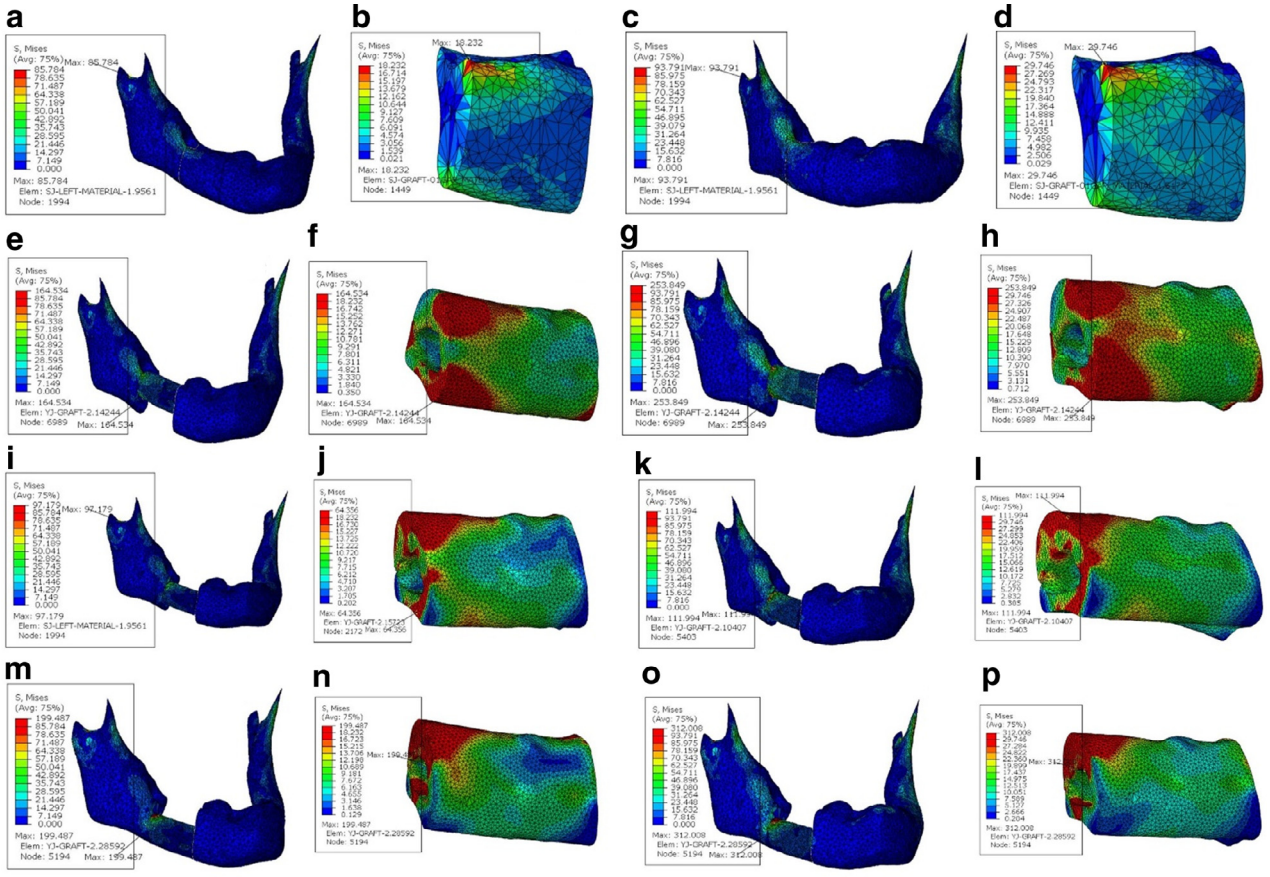

Figure 7 Von Mises stress distribution to the mandible as well as the graft with occlusal loadings. First row: Model I – control group – a and b are loading applied at lower left molar (loading ①), c and d are loading at lower left central incisor(loading ②); second row is Model II; third row is Model III; and fourth row is Model IV. Two left-hand columns are results under loading ① and two right-hand columns are results from loading ②.

Table 3 Maximum Von Mises stress (MPa).

Loading by constraints		Loading ①	Loading ②
Reconstructed mandible	Model I	85.78	93.79
	Model II	164.50	253.80
	Model III	97.18	112.00
	Model IV	199.50	312.00
Fibular graft	Model I	18.23	29.75
	Model II	164.50	253.80
	Model III	64.36	112.00
	Model IV	199.50	312.00

Table 4 Maximum displacement (mm).

Loading by constraints		Loading ①	Loading ②
Reconstructed mandible	Model I	0.704	0.773
	Model II	0.795	0.792
	Model III	0.817	0.801
	Model IV	1.085	1.076
Fibular graft	Model I	0.704	0.529
	Model II	0.718	0.628
	Model III	0.765	0.672
	Model IV	1.035	1.021

Our results showed that stresses always were concentrated at the posterior aspect of the graft and the opposite side of the condyle from the point of loading while maximum displacement occurred at the bone/graft interface. Our previous publication reveals the similar maximum stress and displacement patterns with treatment of mandibular angel fracture.[18] During functional loading to a fractured or reconstructed mandible, the weakest link of the mechanical system of the mandible is the interfragmental gap areas not the TMJ. Therefore, the fixation points of the TMJ were not measured in the study. The measurement of stress and displacement TMJ during functional loading was discussed in our previous study that would not be the key factor for the outcome assessment of the scenario for mandibular reconstruction with fibular graft.[34] Fibula positioned along the inferior border of the mandible always leads to the least desirable mechanical results. Superior positioned graft, intermediate positioned group, and the control group have significantly better results. The same pattern was observed with maximum displacement. Our data show that placing a fibular graft at different vertical positions results in differences in the distribution of stress throughout the

reconstructed mandible, and within the graft itself. The results from this FEM study contribute to the biomechanical understanding of a reconstructed body of the mandible with a fibular graft.

Stress is an essential factor in evaluating the mechanical behavior of mandibular bone. [35,36] Stress distribution in the graft under functional loads is much higher than that in the residual mandibular segments from Models II to IV. The combined average maximum stress from anterior and posterior loads is 10.66 times higher in the mandible with inferiorly positioned graft (Model IV), 8.72 times for superior graft (Model II), and 3.68 times for intermediate graft (Model III) than that of the control group (Model I). Our results show that with combined average maximum stress from anterior and posterior loads is 2.85 times higher in the mandible with inferior positioned graft (Model IV), and 2.33 times of superior graft (Model II) and 1.16 times of intermediate graft (Model III) than that of the control group (Model I). Our results agree with the mechanical principle of one beam theory that stress concentration increases in a small diameter area when forces are applied to a beam system that has one end immobile. A significant discrepancy of stress concentration between the graft and remaining mandibular segments may contribute to the faster resorption rate of a grafted bone (i.e., iliac or others) versus a pristine bone. Fibular grafts are commonly placed at the inferior position because the mandible has the largest diameter at the bottom, which allows the most bone-to-bone contact. Fibular grafts are used for large mandibular defects; therefore, positioning of a reconstruction plate away from dentition along the inferior border rather than using the Champy method is frequently chosen for mandibular reconstruction. Our results show this common practice produces the least desirable mechanical effectiveness.

Cross-sections of fibular bone exhibit a structural pattern that is the opposite of that present in the mandible. The diameter of the fibula has larger width than its vertical height. The fibular segment is usually significantly lower in height than that of the remaining mandible, which creates problems for a later prosthetic restoration of a patient's dentition. The vertical distance between the reconstructed segment and the occlusal plane can be substantially large. This often is a difficult problem for subsequent rehabilitation by an implant-supported prosthesis. The large leverage forces resulting from the high vertical dimension of the prosthetic construction can lead to overloading of the osseointegrated implants and endanger the longevity of the prosthetic restoration.

Based on our results, the height, volume, and shapes of the grafted bone matter suggest that increasing graft volume by methods such as the double-barrel grafts may improve biomechanical properties of the reconstructed mandible for patients who are candidates for later implant-supported dental prostheses. "Double-barrel" grafts are not routinely done because they require more osteotomies and are technically difficult.

One reason for the optimal biomechanics of the graft placed in the intermediate vertical position (Model III) may be that the overall structure of the reconstructed mandible in this case is the most similar to that of the intact mandible. Another reason may be that during chewing the superior part of mandible suffers tensile stress and the inferior part suffers compressive stress; hence, a balance of these forces at an intermediate zone may minimize stress within the graft at this position. A graft placed inferiorly is subjected to great moments stress generated by chewing forces. Thus, a graft placed in the intermediate zone may offer the best biomechanical compromise for the reconstructed mandible that facilitates ease of dental rehabilitation including placement of dental implants and prostheses. The relationship of our results to double-barrel grafts is that the first barrel of full length should be placed at an intermediate to superior position, with the second nonvascularized barrel of shorter length placed either above or below the first barrel as would be most convenient for restorative purposes, as determined by the surgeon.

Even more compellingly, our study supports efforts in developing novel ways of generating bone graft segments of the same size and shape of the original segment, such as by 3D printing of biocompatible metals or polymers as bone analogs would be the new direction for mandibular reconstruction. Future research using FEM and statistical analysis of clinical data, as well as experimental tests, may help to quantify and understand the long term outcome of reconstruction and the restoration of biomechanical function of the reconstructed mandible.

Conclusions

The position of fibular graft placed in the surgical resection site has significant effects on the mechanical behavior of the reconstructed mandible. The fibular graft aligned with the inferior border of the mandible, the most common site designated location by clinicians, has the worst effects on the stress distribution and displacement to the mandibular under functional loads. The fibular graft placed at the intermediate location has the best biomechanics and provides favorable condition for subsequent prosthetic reconstruction. This work provides an important basis for future improvement of the surgical and prosthetic rational for mandibular reconstruction and ultimately the benefits to those patients.

Acknowledgment

This project is supported by the grants from the National Natural Science Foundation of China (Grant no. 51775506), the Natural Science Foundation of Zhejiang Province (Grant no. LY18E050022), and the James Hayward Research Fund.

Conflict of interest

All authors declare that there is no conflict of interest.

References

1. Maciejewski A, Szymczyk C. Fibula free flap for mandible reconstruction: analysis of 30 consecutive cases and quality of life evaluation. *J Reconstr Microsurg* 2007;**23**:1–10.
2. Hidalgo DA. Fibular free flap: a new method of mandible reconstruction. *Plast Reconstr Surg* 1989;**84**:71–9.

3. Wei FC, Seah CS, Tsai YC, et al. Fibular osteoseptocutaneous flap for reconstruction of composite mandibular defects. *Plast Reconstr Surg* 1994;**93**:294–304.
4. Smolka K, Kraehenbuehl M, Eggensperger N. Fibula free flap reconstruction of the mandible in cancer patients: evalution of a combined surgical and prosthodontic treatment concept. *Oral Oncol* 2008;**44**:571–81.
5. Klesper B, Lazar F, Siessegger M, et al. Vertical distraction osteogenesis of fibular transplants for mandibular reconstruction-a preliminary study. *J Craniomaxillofac Surg* 2002;**30**:280–5.
6. Militsakh ON, Werle A, Mohyuddin N, et al. Comparison of radial forearm with fibula and scapula osteocutaneous free flaps for oromandibular reconstruction. *Arch Otolaryngol Head Neck Surg* 2005;**131**:571–5.
7. Lópezarcas JM, Arias J, Del Castillo JL, et al. The fibula osteomyocutaneous flap for mandible reconstruction: a 15-year experience. *J Oral Maxillofac Surg* 2010;**68**:2377–84.
8. Wallace CG, Chang YM, Tsai CY. Harnessing the potential of the free fibula osteoseptocutaneous flap in mandible reconstruction. *Plast Reconstr Surg* 2010;**125**:305–14.
9. Hidalgo DA. Fibula free flap: a new method of mandible reconstruction. *Plast Reconstr Surg* 1989;**84**:71–9.
10. Fujiki M, Miyamoto S, Sakuraba M, et al. A comparison of perioperative complications following transfer of fibular and scapular flaps for immediate mandibular reconstruction. *J Plast Reconstr Aesthet Surg* 2013;**66**:372–5.
11. Wijbenga JG, Schepers RH, Werker PM, et al. A systematic review of functional outcome and quality of life following reconstruction of maxillofacial defects using vascularized free fibula flaps and dental rehabilitation reveals poor data quality. *J Plast Reconstr Aesthetic Surg* 2016;**69**:1024–36.
12. Bezerra TP, Junior S, Scarparo HC, et al. Do erupted third molars weaken the mandibular angle after trauma to the chin region? A 3D finite element study. *Int Illofac Surg* 2013;**42**:474–80.
13. Meyer C, Kahn JL, Boutemi P, et al. Photoelastic analysis of bone deformation in the region of the mandibular condyle during mastication. *J Craniomaxillofac Surg* 2002;**30**:160–9.
14. Kober C, Erdmann B, Lang J, et al. Adaptive finite element simulation of the human mandible using a new physiological model of the masticatory muscles. *Pamm* 2004;**4**:332–3.
15. Antic S, Vukicevic A, Milasinovic M, et al. Impact of the lower third molar presence and position on the fragility of mandibular angle and condyle: A Three-dimensional finite element study. *J Craniomaxillofac Surg* 2015;**43**:870–8.
16. Bujtár P, Sándor GK, Bojtos A, et al. Finite element analysis of the human mandible at 3 different stages of life. *Oral Surg Oral Med Oral Pathol Oral Radiol Endod* 2010;**110**:301–9.
17. Murakami K, Yamamoto K, Sugiura T, et al. Biomechanical analysis of poly-L-lactic acid and titanium plates fixated for mandibular symphyseal fracture with a conservatively treated unilateral condylar fracture using the three-dimensional finite element method. *Dent Traumatol* 2015;**31**:396–402.
18. Wang R, Liu Y, Wang JH, et al. Effect of interfragmentary gap on the mechanical behavior of mandibular angle fracture with three fixation designs: a finite element analysis. *J Plast Reconstr Aesthetic Surg* 2017;**70**:3360–9.
19. Vollmer D, Meyer U, Joos U, et al. Experimental and finite element study of a human mandible. *J Craniomaxillofac Surg* 2000;**28**:91–6.
20. Meyer C, Kahn JL, Lambert A, et al. Development of a static simulator of the mandible. *J Craniomaxillofac Surg* 2000;**28**:278–86.
21. Meyer C, Serhir L, Boutemi P. Experimental evaluation of three osteosynthesis devices used for stabilizing condylar fractures of the mandible. *J Craniomaxillofac Surg* 2006;**34**:173–81.
22. Hart RT, Hennebel VV, Thongpreda N, et al. Modeling the biomechanics of the mandible: a three-dimensional finite element study. *J Biomech* 1992;**25**:261–86.
23. Parashar SK, Sharma JK. A review on application of finite element modeling in bone biomechanics. *Perspect Sci* 2016;**8**:696–8.
24. Tsouknidas A, Anagnostidis K, Maliaris G, et al. Fracture risk in the femoral hip region: a finite element analysis supported experimental approach. *J Biomech* 2012;**45**:1959–64.
25. Khayyeri H, Checa S, Tägil M, et al. Corroboration of mechanobiological simulations of tissue differentiation in an in vivo bone chamber using a lattice-modeling approach. *J Orthop Res* 2009;**27**:1659–66.
26. Rho JY, Hobatho MC, Ashman RB. Relations of mechanical properties to density and CT numbers in human bone. *Med Eng Phys* 1995;**17**:347–55.
27. Rice JC. On the dependence of the elasticity and strength of cancellous bone on the apparent density. *J Biomech* 1998;**2**:155–68.
28. Meyer C, Martin E, Kahn JL, et al. Development and biomechanical testing of a new osteosynthesis plate (TCP) designed to stabilize mandibular condyle fractures. *J Craniomaxillofac Surg* 2007;**35**:84–90.
29. Ramos A, Ballu A, Mesnard M, et al. Numerical and experimental models of the mandible. *Exp Mech* 2011;**51**:1053–9.
30. Vajgel A, Camargo IB, Willmersdorf RB, et al. Comparative finite element analysis of the biomechanical stability of 2.0 fixation plates in atrophic mandibular fractures. *J Oral Maxillofac Surg* 2013;**71**:335–42.
31. Narra N, Valášek J, Hannula M, et al. Finite element analysis of customized reconstruction plates for mandibular continuity defect therapy. *J Biomech* 2014;**47**:264–8.
32. Gregolin RF, Tokimatsu RC, Pereira JA. Biomechanical stress and strain analysis of mandibular human region from computed tomography to custom implant development. *Adv Mater Sci Eng* 2017;**2017**:1–9.
33. Nelson GJ. *Three dimensional computer modeling of human mandibular biomechanics* D.M.D. Thesis. Vancouver: The University of British Columbia; 1986.
34. Liu Y, Wang R, Baur DA, et al. A finite element analysis of the stress distribution to the mandible from impact forces with various orientations of third molars. *J Zhejiang Univ-SC B* 2018;**19**:38–48.
35. Sevimay M, Turhan F, Kiliçarslan MA, et al. Three-dimensional finite element analysis of the effect of different bone quality on stress distribution in an implant-supported crown. *J Prosthet Dent* 2005;**93**:227–34.
36. Shigemitsu R, Yoda N, Ogawa T, et al. Biological-data-based finite-element stress analysis of mandibular bone with implant-supported overdenture. *Comput Bio Med* 2014;**54**:44–52.